Adaptive Twisting Sliding Mode Control for Quadrotor Unmanned Aerial Vehicles

V. T. Hoang, M. D. Phung and Q. P. Ha
Faculty of Engineering and Information Technology, University of Technology Sydney, Australia
E-mail: {VanTruong.Hoang, ManhDuong.Phung, Quang.Ha}@uts.edu.au

***Abstract*—This work addresses the problem of robust attitude control of quadcopters. First, the mathematical model of the quadcopter is derived considering factors such as nonlinearity, external disturbances, uncertain dynamics and strong coupling. An adaptive twisting sliding mode control algorithm is then developed with the objective of controlling the quadcopter to track desired attitudes under various conditions. For this, the twisting sliding mode control law is modified with a proposed gain adaptation scheme to improve the control transient and tracking performance. Extensive simulation studies and comparisons with experimental data have been carried out for a Solo quadcopter. The results show that the proposed control scheme can achieve strong robustness against disturbances while is adaptable to parametric variations within a fixed-time convergence.**

Keywords: **Quadcopter, attitude control, adaptive twisting sliding mode control.**

I. Introduction

Over the last decade, quadcopter unmanned aerial vehicles (UAV) have received much research attention with various applications, ranging from military to industry for surveillance and rescue, civil infrastructure monitoring and inspection. Research on UAVs also covers many areas, including control and planning, data engineering and communication, see. e.g., [1], [2], [3]. While UAV applications continue to growth, a great deal of research effort is being devoted to better handle the control problem of quadcopters, to cope with the complexity of their dynamics, system parameter variations and particularly, large external disturbances. A quadrotor drone has generally six degrees of freedom but only four independent inputs, i.e., the four rotor speeds, thus make it an underactuated system. Besides the coupling condition of rotational and translational motion, the UAV highly nonlinear model is also subject to the aerodynamic effect, which causes microscopic frictions acting on the quadcopter, leading to the need to generate compensative forces to maintain proper movements at steady state. Designing robust control algorithms for quadcopters is therefore an interesting topic.

In the literature, several control algorithms have been developed for quadcopters such as command-filtered PD/PID control [4], integral predictive/H_∞ control [5], optimal control [6], and extended potential field [7]. Among control techniques for UAV, the sliding mode control (SMC) is widely used due to its salient robustness against the influence of modelling errors and external disturbances [1], [8], [9]. In SMC, the chattering effect occuring in the steady state usually excites unmodeled frequencies of the system dynamics. High-order sliding modes (HOSM) based on a higher-order derivatives of the sliding function have been introduced to reduce this effect [10]–[12] and also to improve finite-time convergence [13]. Within the HOSM control, most popular are twisting controllers [14] and their modified versions like super-twisting [15], adaptive twisting [16], and accelerated twisting [17]. Owing to their advantages, these HOSM techniques have been applied to UAV control [18], [19]. However, these control laws are indeed complicated and would require some simpler approach. To this end, the one-stage algorithm of the accelerated twisting sliding mode (ATSM), where the control gain is modified to be always greater than an exponential function of the sliding function magnitude, appears to be simple but can guarantee accelerated finite-time, or at least, fixed-time convergence [17]. Motivated by that work, we propose in this paper an adaptive scheme to adjust the control gain of the twisting control law and apply it to control the attitude of quadcopters in harsh conditions with nonlinearity, external disturbances, uncertain dynamics and strong coupling. The control performance of the proposed controller is verified by simulations and comparisons with real-time data of a Solo drone.

The paper is organised as follows. Section II briefly describes the dynamic model of the quadcopter. Section III presents the design of the proposed adaptive twisting sliding mode controller. Simulation and comparisons with experimental data are introduced in Section IV. The paper ends with a conclusion and recommendation for future work.

II. Dynamic model

The model of the quadcopter used in this work is illustrated in Fig. 1, wherein the inertial frame, (x_E, y_E, z_E), is defined by the ground with the z axis pointing down to the earth centre, and the body frame, (x_B, y_B, z_B), is specified by the orientation of the quadcopter with the z axis pointing upward and the x and y axes pointing to the arms' directions. The translational motion of the quadcopter in the inertial frame is determined by its position, $\xi = (x, y, z)^T$, and velocity, $\dot{\xi} = (\dot{x}, \dot{y}, \dot{z})^T$. The UAV attitude is described by Euler angles roll, pitch, and yaw, $\Theta = (\phi, \theta, \psi)^T$ with the corresponding angular rates $\dot{\Theta} = (\dot{\phi}, \dot{\theta}, \dot{\psi})^T$. Let $\omega = [p, q, r]^T$ be the angular rate of the quadcopter in the inertial frame, i.e.:

$$\omega = \begin{bmatrix} 1 & 0 & -s_\theta \\ 0 & c_\phi & c_\theta s_\phi \\ 0 & -s_\phi & c_\theta c_\phi \end{bmatrix} \dot{\Theta}, \tag{1}$$

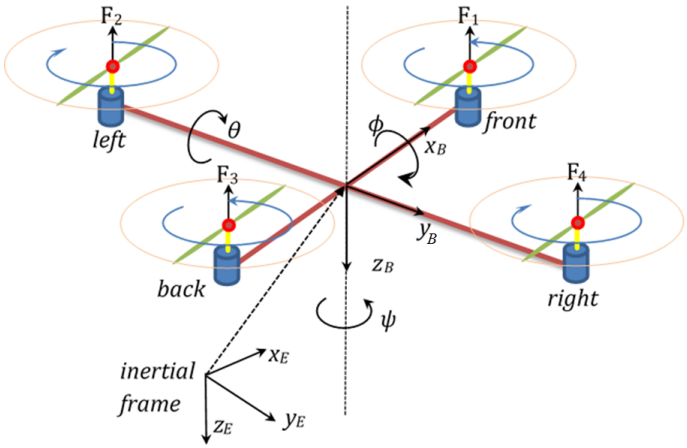

Fig. 1: A schematic diagram of quadcopter

where s_x denotes $sin(x)$ and c_x denote $cos(x)$. The transformation from the body to earth frames is then determined by the following rotation matrix:

$$R = \begin{bmatrix} c_\psi c_\theta & c_\psi s_\theta s_\phi - s_\psi c_\phi & c_\psi s_\theta c_\phi + s_\psi s_\phi \\ s_\psi c_\theta & s_\psi s_\theta s_\phi + c_\psi c_\phi & s_\psi s_\theta c_\phi - c_\psi s_\phi \\ -s_\theta & c_\theta s_\phi & c_\theta c_\phi \end{bmatrix}. \quad (2)$$

Since only the attitude control is concerned in this work, torque components for orientation of the UAV are considered here. They include the torques caused by thrust forces τ, body gyroscopic effects τ_b, propeller gyroscopic effects τ_p, and aerodynamic friction τ_a. Components of the torque vector $\tau = [\tau_\phi \ \tau_\theta \ \tau_\psi]^T$, corresponding to rotation in the roll, pitch and yaw directions, are determined by:

$$\tau_\phi = l(F_2 - F_4), \quad (3)$$
$$\tau_\theta = l(-F_1 + F_3), \quad (4)$$
$$\tau_\psi = c(-F_1 + F_2 - F_3 + F_4), \quad (5)$$

where l is the distance from the motor to the centre of mass of the quadcopter and c is the force-to-torque coefficient. The body gyroscopic torque is determined by:

$$\tau_b = -S(\omega)I\omega, \quad (6)$$

where $S(\omega)$ is a skew-symmetric matrix,

$$S(\omega) = \begin{bmatrix} 0 & -r & q \\ r & 0 & -p \\ -q & p & 0 \end{bmatrix}. \quad (7)$$

The attitude dynamic model of the quadcopter is then described as:

$$I\ddot{\Theta} = \tau_b + \tau + \tau_p - \tau_a, \quad (8)$$

where $I = \text{diag}[I_{xx}, I_{yy}, I_{zz}]$ is the matrix of inertia of the quadrotor, assumed to be symmetrical.

In our system, the gyroscopic and aerodynamic torques are considered as external disturbances. Thus, the control inputs mainly depend on torque τ and from (3), (4) and (5), they can be represented as:

$$\begin{bmatrix} u_\phi \\ u_\theta \\ u_\psi \\ u_z \end{bmatrix} = \begin{bmatrix} \tau_\phi \\ \tau_\theta \\ \tau_\psi \\ F \end{bmatrix} = \begin{bmatrix} 0 & l & 0 & -l \\ -l & 0 & l & 0 \\ -c & c & -c & c \\ 1 & 1 & 1 & 1 \end{bmatrix} \begin{bmatrix} F_1 \\ F_2 \\ F_3 \\ F_4 \end{bmatrix}, \quad (9)$$

where F is the UAV lift, u_z represents the total thrust acting on the four propellers and u_ϕ, u_θ and u_ψ respectively represent the roll, pitch and yaw torques. As only the attitude of quadcopter will be controlled, u_z is assumed to balance with the gravity. Therefore, the second-order nonlinear dynamic equations of the quadcopter for attitude control can be described by:

$$\ddot{\phi} = \frac{I_{yy} - I_{zz}}{I_{xx}} qr + \frac{1}{I_{xx}} u_\phi + d_\phi \quad (10)$$
$$\ddot{\theta} = \frac{I_{zz} - I_{xx}}{I_{yy}} pr + \frac{1}{I_{yy}} u_\theta + d_\theta \quad (11)$$
$$\ddot{\psi} = \frac{I_{xx} - I_{yy}}{I_{zz}} pq + \frac{1}{I_{zz}} u_\psi + d_\psi, \quad (12)$$

where d_ϕ, d_θ and d_ψ are angular acceleration disturbances.

Then, the quadcopter dynamics can be represented as follows:

$$\begin{cases} \dot{X}_1 = X_2 \\ \dot{X}_2 = f(X) + g(X)u + d(t), \end{cases} \quad (13)$$

where $X_1 = \Theta$, $X_2 = \dot{\Theta}$, $X = [X_1, X_2]^T$ is the state vector, $u = [u_\phi, u_\theta, u_\psi]^T$ is the input vector, $d(t) = [d_\phi, d_\theta, d_\psi]^T$ is the disturbance vector, $g(X) = I^{-1}$, and $f(X)$ is the matrix represented as

$$f(X) = \begin{pmatrix} a_1 qr \\ a_2 pr \\ a_3 pq \end{pmatrix}, \quad (14)$$

where $a_1 = \frac{I_{yy} - I_{zz}}{I_{xx}}, a_2 = \frac{I_{zz} - I_{xx}}{I_{yy}}, a_3 = \frac{I_{xx} - I_{yy}}{I_{zz}}$.

In our system, the following assumptions are made:

A.1 The quadcopter structure is rigid and symmetric.

A.2 The reference trajectories and their first and second time derivatives are bounded.

A.3 The velocity and the acceleration of the quadcopter are bounded.

A.4 The orientation angles are limited to $\phi \in \left[-\frac{\pi}{2}, \frac{\pi}{2}\right]$, $\theta \in \left[-\frac{\pi}{2}, \frac{\pi}{2}\right]$ and $\psi \in [-\pi, \pi]$.

III. Control Design

Given the desired angle reference $X_{1d} = \{\phi_d, \theta_d, \psi_d\}^T$, the overall control law is presented as

$$u(t) = u_{eq}(t) + u_D(t), \quad (15)$$

where $u_{eq}(t) = (u_{eq,i})^T$ and $u_D(t) = (u_{D,i})^T$, $i = 1, 2, 3$, are respectively the equivalent control and the discontinuous part containing switching elements. In our system, the sliding surface equation is chosen as:

$$\sigma = \dot{\mathbf{e}} + \Lambda \mathbf{e}, \quad (16)$$

where $\Lambda = \text{diag}(\lambda_\phi, \lambda_\theta, \lambda_\psi)$ is a positive definite matrix being designed, and $\mathbf{e}$ is the control error, $\mathbf{e} = X_{1d} - X_1$.

1) Design u_{eq}: The equation (16) can be rewritten for the attitude sliding surface as:

$$\sigma = (\dot{X}_{1d} - \dot{X}_1) + \Lambda(X_{1d} - X_1). \tag{17}$$

Taking the time derivative of σ, we have:

$$\dot{\sigma} = (\ddot{X}_{1d} - \ddot{X}_1) + \Lambda(\dot{X}_{1d} - \dot{X}_1), \tag{18}$$

or

$$\dot{\sigma} = \ddot{X}_{1d} - \dot{X}_2 + \Lambda\dot{e}. \tag{19}$$

Substitute $\ddot{X}$ from (13) to (19) yields:

$$\dot{\sigma} = \ddot{X}_{1d} - \big[f(X) + g(X)u\big] + \Lambda\dot{e}. \tag{20}$$

When the sliding mode has been induced, u can be considered as the equivalent control u_{eq}. By driving the derivative of sliding surface to zero, the equivalent control rule is computed as follows:

$$u_{eq} = g(X)^{-1}\left(\ddot{X}_{1d} - f(X) + \Lambda\dot{e}\right). \tag{21}$$

2) Design u_D: The discontinuous control is

$$u_D = g(X)^{-1}u_T, \tag{22}$$

where the twisting controllers $u_{T,i},\ i = 1, 2, 3$ are adopted here as:

$$u_{T,i} = \begin{cases} -\mu_i\alpha_i\text{sign}(\sigma_i) & \text{if } \sigma_i\dot{\sigma}_i \le 0 \\ -\alpha_i\text{sign}(\sigma_i) & \text{if } \sigma_i\dot{\sigma}_i > 0, \end{cases} \tag{23}$$

where $\mu_i < 1$ is a fixed positive number and α_i is the control gain [10]. To improve the control transient and tracking performance, the gain α_i in (23) could be selected to satisfy the following condition for the one-stage accelerated twisting algorithm [17]:

$$\alpha_i = \max\{\alpha_{*,i}, \gamma_i|\sigma_i|^{\rho_i}\}, \tag{24}$$

where $\alpha_{*,i}$, γ_i and ρ_i are positive constants. Given that fixed time stability is required over a large operational region of the UAV, and motivated by the simplicity of the one-stage accelerated twisting algorithm mentioned above, we propose here to adjust the gain α_i in (23) with an adaptive one [19], [20], constructed based on the following equation:

$$\dot{\alpha}_i = \begin{cases} \bar{\omega_i}\big|\sigma_i(\omega, t)\big|\,\text{sign}(|\sigma_i(\omega, t)|^{\rho_i} - \epsilon_i) & \text{if } \alpha_i > \alpha_{m,i} \\ \eta_i & \text{if } \alpha_i \le \alpha_{m,i}, \end{cases} \tag{25}$$

where $\bar{\omega_i}, \rho_i > 0$, ϵ_i and η_i are positive constants and $\alpha_{m,i}$ is an adaptation threshold, chosen to be greater than $\alpha_{*,i}$.

To prove the convergence of the proposed control and adaptation schemes, let us consider the Lyapunov function candidate:

$$V = \frac{1}{2}\sigma^T I\sigma + \sum_{i=1}^{3}\frac{1}{2\gamma_i}(\alpha_i - \alpha_{M,i})^2, \tag{26}$$

where I is the inertia matrix,γ_i is a positive constant, and $\alpha_{M,i}$ is the maximum value of the adaptive gain, i.e. $0 < \alpha_{m,i} < \alpha < \alpha_{M,i}$. According to A.1, $\dot{I} = 0$. Thus, by taking the time derivative of V and substituting $\dot{\sigma}$ from (20), one has

$$\begin{aligned} \dot{V} =& \sigma^T I\dot{\sigma} + \sum_{i=1}^{3}\frac{1}{\gamma_i}(\alpha_i - \alpha_{M,i})\dot{\alpha}_i \\ =& \sigma^T\left(-I\ddot{X}_{1d} + I\Lambda\dot{e} - S(\omega)I\omega + Iu + d\right) \\ &+ \sum_{i=1}^{3}\frac{1}{\gamma_i}(\alpha_i - \alpha_{M,i})\dot{\alpha}_i. \end{aligned} \tag{27}$$

Assuming that the disturbance d is bounded, i.e., $|d_i| \le \Xi_{M,i}$ and equation (27) becomes

$$\begin{aligned} \dot{V} &= \sigma^T(d + u_T) + \sum_{i=1}^{3}\frac{1}{\gamma_i}(\alpha_i - \alpha_{M,i})\dot{\alpha}_i \\ &= \sum_{i=1}^{3}\left[\sigma_i(d_i + u_{T,i}) + \frac{1}{\gamma_i}(\alpha_i - \alpha_{M,i})\dot{\alpha}_i\right]. \end{aligned} \tag{28}$$

For the case $\sigma_i\dot{\sigma}_i \le 0$, from the twisting control law, we have

$$\begin{aligned} \dot{V} =& \sum_{i=1}^{3}\sigma_i\left[d_i - \alpha_i\mu_i\text{sign}(\sigma_i)\right] + \\ &+ \sum_{i=1}^{3}\frac{1}{\gamma_i}(\alpha_i - \alpha_{M,i})\bar{\omega}_i|\sigma_i|\,\text{sign}(|\sigma_i|^{\rho_i} - \epsilon_i) \\ =& \sum_{i=1}^{3}|\sigma_i|\,\mu_i\Big[\frac{d_i\text{sign}(\sigma_i)}{\mu_i} - \alpha_i \\ &+ \frac{\bar{\omega}_i}{\gamma_i\mu_i}(\alpha_i - \alpha_{M,i})\text{sign}(|\sigma_i|^{\rho_i} - \epsilon_i)\Big]. \end{aligned} \tag{29}$$

Thus, with sufficiently small ϵ_i such that $|\sigma_i|^{\rho_i} > \epsilon_i$ [20], then $\dot{V} \le 0$ if

$$\left|\frac{d_i\text{sign}(\sigma_i)}{\mu_i}\right| \le \alpha_i \text{ or } \alpha_i \ge \frac{\Xi_i}{\mu_i}. \tag{30}$$

Note that the case $\alpha_i > \alpha_{m,i}$ is considered here only as otherwise the last term in the right hand side of (29) becomes $\frac{1}{\gamma_i}(\alpha_i - \alpha_{M,i})\eta_i < 0$, which is straightforward. For the case $\sigma_i\dot{\sigma}_i > 0$, from (23) we can have the same result as above if considering $\mu_i = 1$.

IV. Simulation and Validation

Extensive simulations and comparison has been conducted to evaluate the performance of the proposed controller. The quadcopter model used for in this study is the 3DR Solo drone, shown in Fig. 2. The UAV is equipped with a laser scanner, camera, and three processors, two are Cortex M4 168 MHz running Pixhawk firmware for low-level control and the other is an ARM Cortex A9 running Arducopter flight operating system. The programming is carried out through the ground control station called Mission Planner and uploaded to the UAV [19]. Its parameters are listed in Table I with detailed measurements obtained therein. Control parameters are given in Table II.

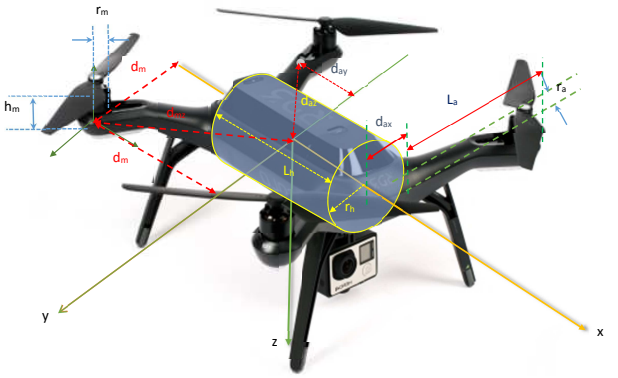

Fig. 2: The 3DR Solo drone with body coordinate frame.

TABLE I: Parameters of the quadcopter model

Parameter	Value	Unit
m	1.50	kg
l	0.205	m
g	9.81	m/s^2
I_{xx}	$8.85 \cdot 10^{-3}$	$kg.m^2$
I_{yy}	$15.5 \cdot 10^{-3}$	$kg.m^2$
I_{zz}	$23.09 \cdot 10^{-3}$	$kg.m^2$

TABLE II: Control design parameters

Variable	Value	Variable	Value
λ_1, λ_2	4.68	$\gamma_{a,1}, \gamma_{a,2}, \gamma_{a,3}$	6.6
λ_3	3.84	ρ_1, ρ_2, ρ_3	3
μ_1, μ_2, μ_3	0.3	$\epsilon_1, \epsilon_2, \epsilon_3$	0.6
$\alpha_{M,1}, \alpha_{M,2}$	2.001	$\alpha_{m,1}, \alpha_{m,2}$	0.01
$\alpha_{M,3}$	2.002	$\alpha_{m,3}$	0.02
$\omega_1, \omega_2, \omega_3$	200	η_1, η_2, η_3	0.01

A. *Control performance in nominal conditions*

We first evaluate the performance of the controller in nominal conditions. In this case, the quadcopter is assumed to be in steady state at a hovering condition where all attitude angles and angular velocities are zeros. New reference angles are then provided with the values $\phi = -10°$, $\theta = 10°$ and $\psi = 45°$ at time 0.5 s, 1 s and 2 s, respectively. The system responses and controller outputs are shown in Fig. 3 and Fig. 4, respectively, where in the latter the time scale is zoomed in to observe the abrupt change in references and coupling effects. It can be seen that the proposed controller smoothly drives the angles to the reference values within one second and with a small overshoot despite strong coupling relations among control variables as described in Eqs. (10-12).

B. *Responses to disturbances*

In this simulation, we evaluated robustness of the controller by adding disturbances with the mean value of 0.5 Nm to the torques in all three body axes of the quadcopter. Reference values were selected to be the same as in previous simulations. Results are shown in Fig. 5. It can be seen that the proposed

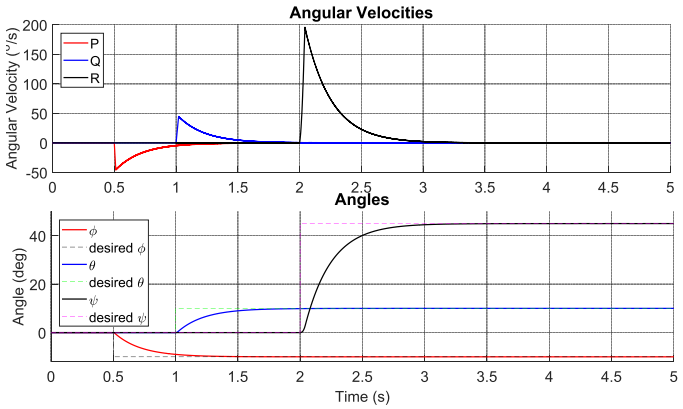

Fig. 3: Responses of the quadcopter in nominal conditions (P, Q and R- roll, pitch and yaw angular velocities).

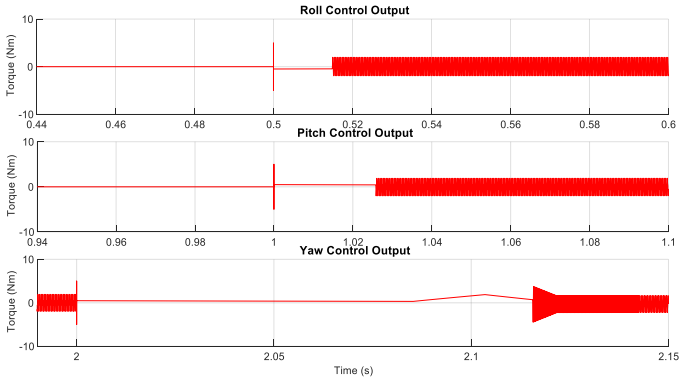

Fig. 4: Control torques.

controller effectively rejects the disturbances to drive the quadcopter to reach the expected attitude within a similar time period as in nominal conditions.

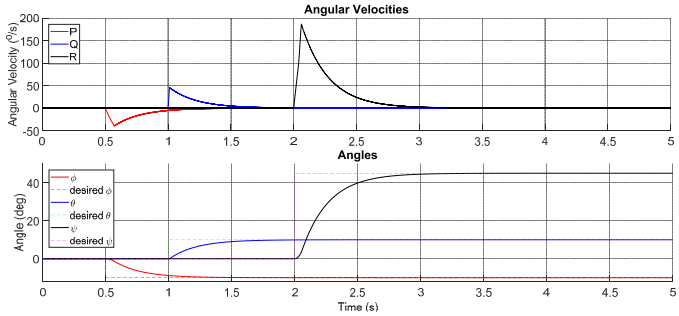

Fig. 5: Angular velocity and angle responses in the presence of disturbances.

C. *Responses to parametric variations*

In this simulation, the quadrotor is subject to several sources of uncertainties including variations in loads and moments of inertia. Specifically, a load of 0.8 kg, the largest load the 3DR Solo quadcopter can carry, was added to the model together with the following uncertainties in moments of inertia:

$$\Delta I = \begin{bmatrix} 0 & 0.0044 & -0.0077 \\ 0.0044 & 0 & 0.0115 \\ -0.0077 & 0.0115 & 0 \end{bmatrix}. \quad (31)$$

Figure 6 shows the results in comparison with the nominal conditions. The settling time and overshoot between responses are almost identical, indicating the robustness of the proposed controller. The variation of adaptive gain $\alpha_1(t)$ is shown in Fig. 7. Higher gain magnitudes observed in the two sub-figures imply more energy was required to stabilise the system to cope with the increase in disturbances and uncertainties owing to the effectiveness of the adaptation.

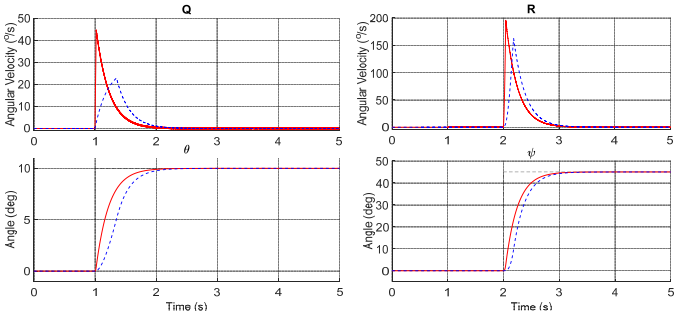

Fig. 6: Angle and angular velocity responses in the presence of parametric variations.

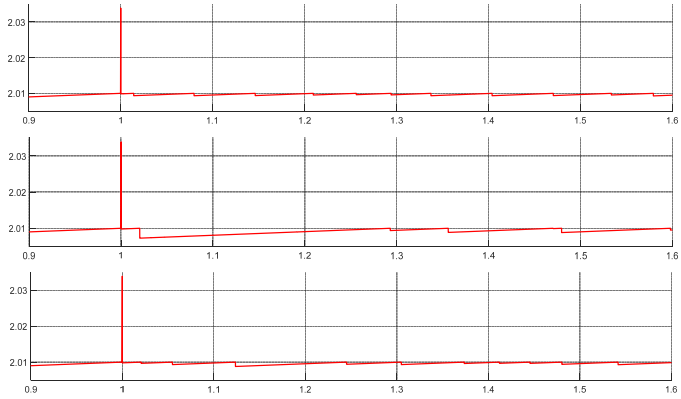

Fig. 7: The adaptation of gain $\alpha_1(t)$ in different scenarios.

Fig. 8: Experiment data

D. Comparison and validation with real-time data

For evaluation of the proposed control approach, simulation results were compared with real-time data obtained by using

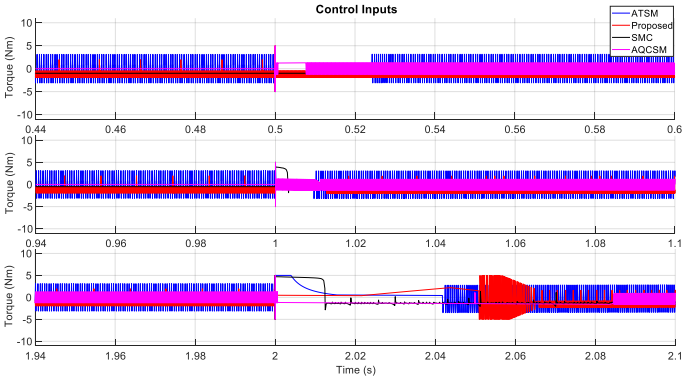

Fig. 9: Time responses of three control inputs.

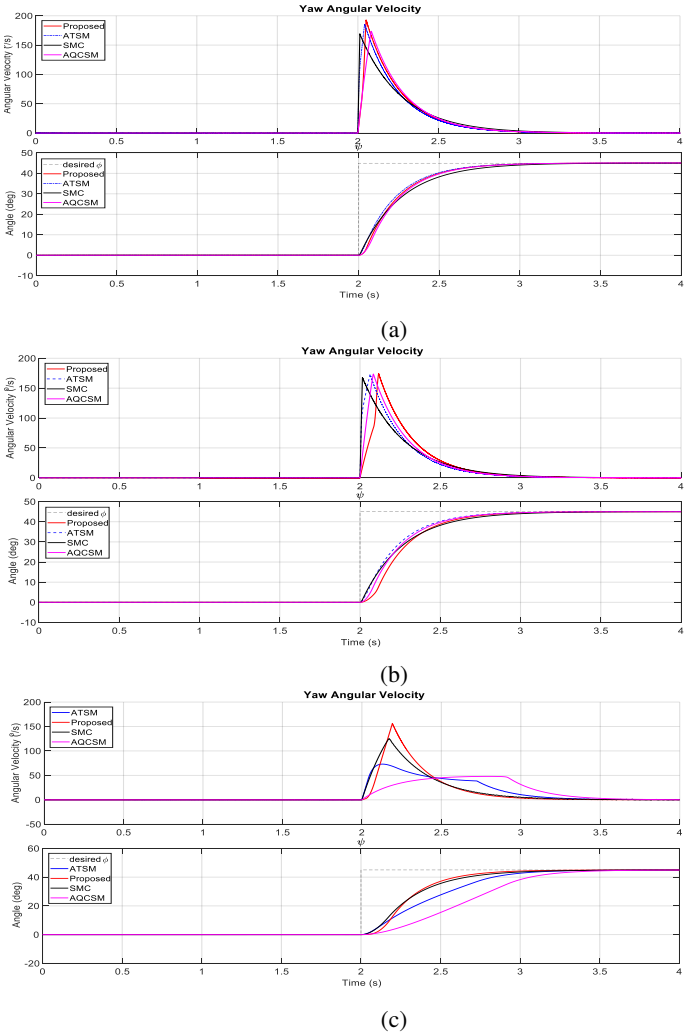

(a)

(b)

(c)

Fig. 10: The yaw angle and yaw angular velocity responses of controllers in three scenarios:
(a) Nominal condition; (b) Occurrence of disturbances; and (c) Parametric variations.

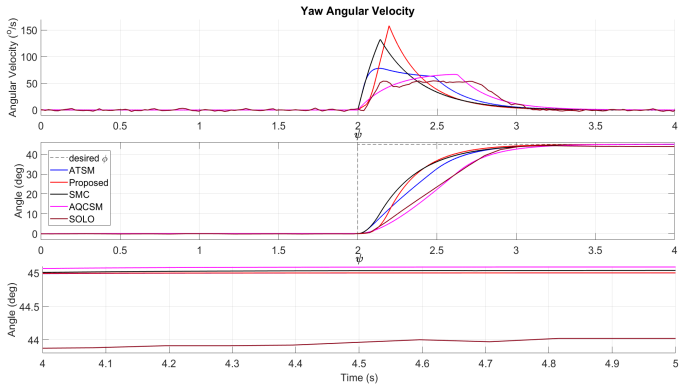

Fig. 11: Zoom-in tracking errors of controllers at the steady state.

the built-in PID controller of the 3DR Solo drone to perform the attitude control. Figure 8 shows the flying path and data recorded, omitting position information, during the experiment.

To compare the performance of the proposed controller with other techniques, its output responses were compared with those responses obtained by using the conventional SMC, the adaptive quasi-continuous (AQCSM) [19] and the accelerated twisting sliding mode (ATSM) [17]. The comparison were conducted under scenarios similar to the ones described in Section IV-A, IV-B and IV-C. Also, for the validation purpose, simulation results were compared with real-time data obtained by using the built-in PID controller of the 3DR Solo drone when performing some attitude control tasks. These results are shown in Fig. 9 for the three control torques, where the proposed controller results in better tracking performance with reduced chattering. Indeed, Fig. 10 shows the time responses of yaw angle and angular velocity wherein their tracking errors at steady state are zoomed in Fig. 11. It can be seen that all controllers show similar performance in nominal conditions. In the presence of disturbances, the proposed controller can however exhibit smallest tracking errors, indicating a better capability in dealing with disturbances. In the case of parametric variation, the proposed controller can also provide the fastest convergence thanks to our proposed adaptive scheme.

V. Conclusion

In this paper, we have proposed an adaptive twisting sliding mode approach for robust control of quadcopter UAV. The proposed controller is a modification of the accelerated twisting sliding mode control with an adaptive scheme to adjust the discontinuous gain to deal with not only external disturbances but also parametric variations. The performance of the controller was evaluated and compared with other controllers in various simulation scenarios. Its validity was also confirmed by comparing with experimental real-time data. Future plan will focus on implementing the proposed controller to enable higher level tasks of the drone such as cooperative tracking and visual inspection.

References

[1] L. Derafa, A. Benallegue, and L. Fridman, "Super twisting control algorithm for the attitude tracking of a four rotors uav," *Journal of the Franklin Institute*, vol. 349, no. 2, pp. 685–699, 2012.

[2] S. Rajappa, C. Masone, H. Bulthoff, and P. Stegagno, "Adaptive super twisting controller for a quadrotor uav," in *Robotics and Automation (ICRA), 2016 IEEE International Conference on*. IEEE, 2016, pp. 2971–2977.

[3] M. Phung, C. Quach, T. Dinh, and Q. Ha, "Enhanced discrete particle swarm optimization path planning for uav vision-based surface inspection," *Automation in Construction*, vol. 81, pp. 25–33, 2017.

[4] Z. Zuo, "Trajectory tracking control design with command-filtered compensation for a quadrotor," *IET Control Theory Appl.*, vol. 4, no. 11, pp. 2343–2355, 2010.

[5] G. V. Raffo, M. G. Ortega, and F. R. Rubio, "An integral predictive/nonlinear H_∞ control structure for a quadrotor helicopter," *Automatica*, vol. 46, no. 1, pp. 29–39, 2010.

[6] R. Ritz, M. Hehn, S. Lupashin, and R. D'Andrea, "Quadrocopter performance benchmarking using optimal control," in *Intelligent Robots and Systems (IROS), 2011 IEEE/RSJ International Conference on*, Sept 2011, pp. 5179–5186.

[7] A. Woods, H. M. La, and Q. P. Ha, "A novel extended potential field controller for use on aerial robots," in *Automation Science and Engineering (CASE), 2016 IEEE International Conference on*, 2016, pp. 286–291.

[8] R. Xu and Ü. Özgüner, "Sliding mode control of a quadrotor helicopter," in *Decision and Control, 2006 45th IEEE Conference on*. IEEE, 2006, pp. 4957–4962.

[9] L. Besnard, Y. B. Shtessel, and B. Landrum, "Control of a quadrotor vehicle using sliding mode disturbance observer," in *American Control Conference, 2007. ACC'07*. IEEE, 2007, pp. 5230–5235.

[10] A. Levant, "Sliding order and sliding accuracy in sliding mode control," *International journal of control*, vol. 58, no. 6, pp. 1247–1263, 1993.

[11] M. Manceur, N. Essounbouli, and A. Hamzaoui, "Second-order sliding fuzzy interval type-2 control for an uncertain system with real application," *Fuzzy Systems, IEEE Transactions on*, vol. 20, no. 2, pp. 262–275, 2012.

[12] G. J. Rubio, J. M. Cañedo, V. I. Utkin, and A. G. Loukianov, "Second order sliding mode block control of single-phase induction motors," *International Journal of Robust and Nonlinear Control*, vol. 24, no. 4, pp. 682–698, 2014.

[13] V. Utkin, "Discussion aspects of high-order sliding mode control," *IEEE Transactions on Automatic Control*, vol. 61, no. 3, pp. 829–833, 2016.

[14] A. Polyakov and A. Poznyak, "Lyapunov function design for finite-time convergence analysis:twisting controller for second-order sliding mode realization," *Automatica*, vol. 45, no. 2, pp. 444–448, 2009.

[15] ——, "Reaching time estimation for super-twisting second order sliding mode controller via lyapunov function designing," *IEEE Transactions on Automatic Control*, vol. 54, no. 8, pp. 1951–1955, 2009.

[16] Y. Shtessel, M. Taleb, and F. Plestan, "A novel adaptive-gain supertwisting sliding mode controller: methodology and application," *Automatica*, vol. 48, no. 5, pp. 759–769, 2012.

[17] Y. Dvir and A. Levant, "Accelerated twisting algorithm," *IEEE Transactions on Automatic Control*, vol. 60, no. 10, pp. 2803–2807, 2015.

[18] E.-H. Zheng, J.-J. Xiong, and J.-L. Luo, "Second order sliding mode control for a quadrotor uav," *ISA transactions*, vol. 53, no. 4, pp. 1350–1356, 2014.

[19] V. T. Hoang, A. M. Singh, M. D. Phung, and Q. P. Ha, "Adaptive second-order sliding mode control of uavs for civil applications," in *Automation and Robotics in Construction (ISARC), 2017 International Symposium on*, 2017.

[20] F. Plestan, Y. Shtessel, V. Bregeault, and A. Poznyak, "New methodologies for adaptive sliding mode control," *International journal of control*, vol. 83, no. 9, pp. 1907–1919, 2010.